

Reduction of the Long-Term Inaccuracy from the AVHRR–Based NDVI Data

Md. Z. Rahman¹, Leonid Roytman², and M. Nazrul Islam³

¹LaGuardia Community College, New York, NY 11101, USA

²NOAA-CREST, The City College of New York, New York, NY 10031, USA

³State University of New York, Farmingdale, NY

Email: zrahman@lagcc.cuny.edu; royman@ccny.cuny.edu; islamm@farmingdale.edu

Abstract—This paper investigated the normalized difference vegetation index (NDVI) stability in the NOAA/NESDIS Global Vegetation Index (GVI) data during 1982-2003, which was collected from five NOAA series satellites. An empirical distribution function (EDF) was developed to eliminate the long-term inaccuracy of the NDVI data derived from the AVHRR sensor on NOAA polar orbiting satellite. The instability of data results from orbit degradation as well as from the circuit drifts over the life of a satellite. Degradation of NDVI over time and shifts of NDVI between the satellites were estimated using the China data set, because it includes a wide variety of different ecosystems represented globally. It was found that the data for the years of 1988, 1992, 1993, 1994, 1995 and 2000 are not stable compared to other years because of satellite orbit drift, AVHRR sensor degradation, and satellite technical problems, including satellite electronic and mechanical satellite systems deterioration. The data for NOAA-7(1982, 1983), NOAA-9 (1985, 1986), NOAA-11(1989, 1990), NOAA-14(1996, 1997), and NOAA-16 (2001, 2002) were assumed to be standard because the crossing time of satellite over the equator (between 1330 and 1500 hours) maximized the value of the coefficients. These years were considered as the standard years, while in other years the quality of satellite observations significantly deviated from the standard. The deficiency of data for the affected years were normalized or corrected by using the method of EDF and comparing with the standard years. These normalized values were then utilized to estimate new NDVI time series which show significant improvement of NDVI data for the affected years.

Index Terms—NDVI, AVHRR, satellite, orbit, drift, empirical distribution function

I. INTRODUCTION

For approximately last three decades, the advanced very high resolution radiometer (AVHRR) on NOAA polar-orbiting satellites have been observing radiances, which have been collected, sampled, and stored for the entire world [1]-[3]. These data were intensively being used by the global community for studying and monitoring land surface, atmosphere, and lately for analyzing climate and environmental changes [4], [5]. AVHRR data, though informative, cannot be directly used in climate change studies because of the orbit drift

in the NOAA satellites (particularly, NOAA-9, -11, and -14) over these satellites' life time [2], [3], [6]-[9]. Devasthale et al. [3] and Price [7] attributed this drift to the selection of a satellite orbit designed to avoid direct sunshine on the instruments. This orbital drift leads to the measurements of normalized difference vegetation index (NDVI) being taken at different local times during the satellites' life time, thereby introducing a temporal inconsistency in the NDVI data [3], [7], [8]. Consequently, a declining trend results in the NDVI data calculated by some satellites.

The objective of this paper is to investigate the NDVI stability in the NOAA/NESDIS global vegetation index (GVI) data for the period of 1982-2003 [10]. AVHRR weekly data for the five NOAA afternoon satellites, namely, NOAA-7, NOAA-9, NOAA-11, NOAA-14, and NOAA-16, were used for the China data set, because it includes a wide variety of different ecosystems represented globally. It was found during investigation that data for the years of 1988, 1992, 1993, 1994, 1995 (first eight weeks), and 2000 are not stable compared to other years because of satellite orbit drift, AVHRR sensor degradation, and satellite technical problems, including satellite electronic and mechanical satellite systems deterioration and failure. Therefore, the data for NOAA-7(1982, 1983), NOAA-9 (1985, 1986), NOAA-11(1989, 1990), NOAA-14(1996, 1997), and NOAA-16 (2001, 2002) were assumed to be standard because the crossing time of satellite over the equator (between 1330 and 1500 hours) maximized the value of the coefficients, and these years were termed as the standard years. In other years, the quality of satellite observations was found to significantly deviate from the standard. This paper proposes a novel scientific methodology that can be easily implemented to generate the desired long-term time-series. The goal of proposed method is to correct the NDVI data calculated from the AVHRR observations for the years of 1988, 1992, 1993, 1994, 1995, and 2000 by employing an empirical distribution function (EDF) compared to the standard data. The proposed methodology can as well be applied to create a global vegetation index in order to improve climatology. The data sets corrected by the proposed method can be used as a proxy to study climate change, epidemic analysis, drought prediction and similar applications.

Manuscript received July 24, 2014; revised November 25, 2014.
Corresponding author email: islamm@farmingdale.edu.
doi:10.12720/jcm.9.11.821-828

II. AREA UNDER INVESTIGATION

For investigation of this paper, we wanted to select an area with diverse ecosystems. China has all the major types of ecosystems present in the world, and therefore, the current study investigated the NDVI stability over China. It also reduces the amount of data to a manageable state and captures global variety of ecosystems in a single geographic region.

China is located in central Asia between 28° N to 43° N in latitude and 75° E to 123° E in longitude. It is bound by Mongolia, Russia and Kazakhstan to the north, North Korea, the Yellow Sea and the East China Sea to the east, the South China Sea, the Gulf of Tonkin, Vietnam, Laos, Myanmar, India, Bhutan and Nepal to the south as well as India, Afghanistan, Pakistan, Tajikistan and Kyrgyzstan to the west. Over 66% of China is upland hill, mountains, and plateau. The highest mountains and plateau are found to the west. To the north and east of the Tibetan Plateau, the land decreases to the desert or semi-desert areas of Sinkiang and Inner Mongolia. To the northeast side, the broad fertile Manchurian Plains are separated from North Korea by the densely forested uplands of Changpai Shan. East of the Tibetan Plateau and south of Inner Mongolia is the Sichuan Basin, which is drained by the Yangtze River that flows east across the southern plains to the East China Sea. The southern plains along the east coast of China have rich, fertile soils and are protected from the north winds. Both Hong Kong and Macau are enclosed on the southeast coast.

III. NORMALIZED DIFFERENCE VEGETATION INDEX

To determine the density of green on a patch of land, it needs to observe the distinct colors (wavelengths) of visible and near-infrared sunlight reflected by the plants. The pigment in plant leaves, chlorophyll, strongly absorbs the visible light (from 0.4 to 0.7 μm) for use in photosynthesis. The cell structure of the leaves, on the other hand, strongly reflects the near-infrared light (from 0.7 to 1.1 μm).

The NOAA AVHRR instrument has five detectors, two of which are sensitive to the wavelengths of light ranging from 0.58–0.68 and 0.725–1.0 micrometers. AVHRR's detectors can be utilized to measure the intensity of light coming off the Earth in visible and near-infrared wavelengths and to quantify the photosynthetic capacity of the vegetation in a given pixel (an AVHRR pixel is 4 square km) of land surface. Nearly all satellite vegetation indices employ this difference formula to quantify the density of plant growth on the Earth-near-infrared radiation minus visible radiation, divided by near-infrared radiation plus visible radiation. The reflectance measured from Channel 1 (visible: 0.58 - 0.68 microns) and Channel 2 (near infrared: 0.725 - 1.0 microns) are used to calculate the index as given by

$$\text{NDVI} = \frac{(\text{Ch2} - \text{Ch1})}{(\text{Ch2} + \text{Ch1})} \quad (1)$$

NDVI typically ranges from 0.1 to 0.6, with higher values representing canopy. Surrounding soil and rock values are close to zero; while the differential for water bodies, such as, rivers and dams, have the opposite trend to vegetation and the index is negative. A range of errors, such as, scattering by dust and aerosols, Rayleigh scattering, subpixel-sized clouds, plus large solar zenith angles and large scan angles, all act to increase Ch1 with respect to Ch2 and hence reduce the computed NDVI [5], [11].

IV. DATA SET

Satellite data were presented bi-weekly with NDVI collected from the NOAA GVI data [10] for the years of 1982 to 2003. The GVI was developed from the reflectance/emission observed by the AVHRR of NOAA polar-orbiting satellite in the visible (VIS), near infrared (NIR) and infrared (IR) wavelength [10]. In developing the GVI, the measurements were spatially sampled from 4 km² (global area coverage) to 16 km² and from daily observations to seven-day composite observations. The VIS and NIR reflectance were pre- and post-launch calibrated and NDVI was calculated as given by

$$\text{NDVI} = \frac{(\text{NIR} - \text{VIS})}{(\text{NIR} + \text{VIS})} \quad (2)$$

NDVI has a high frequency noise related to the variable transparency of the atmosphere, bidirectional reflectance, and orbital drift, which makes it difficult to use the parameter in the analysis. The noise was removed from the data by applying statistical techniques to NDVI time series [5], [12]. The 1982-2003 weekly NDVI data were collected for each 16 km² pixel of the China data set, because it includes a wide variety of different ecosystems such as desert, forest and grassland, which represent the global ecosystem. The weekly GVI data from January 1982 through January 1985 for NOAA-7, from April 1985 through September 1988 for NOAA-9, from October 1988 through August 1994 for NOAA-11, from March 1995 through December 2000 for NOAA-14, and from January 2001 through December 2003, for NOAA-16, were used in this paper.

V. PROPOSED METHODOLOGY

For each satellite, we constructed the NDVI time series and also approximated the linear trend using the least square technique. From trend equation, we estimated two values, namely, the largest difference (dN_i) between NDVI at the beginning (N_b) and the end (N_e) of satellite life, and difference (dN_s) between NDVI at the beginning of the next (n) satellite (N_{bn}) and at the end of the previous (p) one (N_{ep}). Both differences were normalized in order to compare NDVI performance for different ecosystems [5] as described below.

$$dN_t = 100 \left(\frac{N_e - N_b}{N_b} \right) \quad (3)$$

$$dN_s = 100 \left(\frac{N_{bn} - N_{ep}}{N_{ep}} \right) \quad (4)$$

The NDVI time series has upward trend when the dN_t is positive and downward when it is negative value. The parameter, dN_s determines the magnitude of NDVI such that a positive value indicates larger NDVI at the end of the previous satellite and a negative value indicates smaller NDVI.

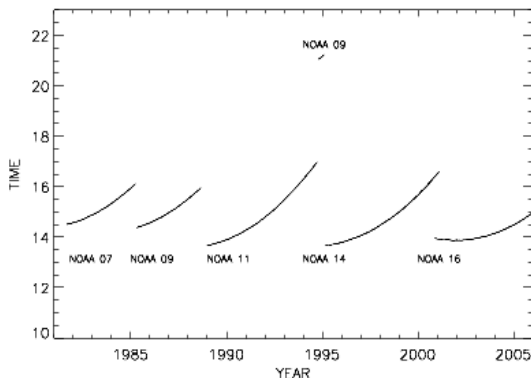


Fig. 1. Equator crossing times for NOAA-7, -9, -11, -14 and -16 [13]

To the best knowledge of the authors, there has been no physical or analytical method available in the literature that can be used to correct for the stability of NDVI. The paper developed a statistical model for the correction of NDVI By using an empirical distribution function (EDF). The function was used to generate normalized data for the years of 1988, 1992, 1993, 1994, 1995 and 2000 compared with standard years' data. Data for the years of 1982, 1983, 1985, 1986, 1989, 1990, 1996, 1997, 2001, and 2002 can be used as the standards for other years, as the crossing time of satellite over the equator (between 1330 and 1500 hours) as shown in Fig. 1 [13]. This process maximizes the value of coefficients. In other years, the quality of satellite observations significantly deviates from the standard. Also the data from the afternoon passes of the satellites are affected by a drift to 1-2 hours or delay in local overpass time, during a nominal three-four year life time [3], [7]. Image data from the AVHRR slowly shifts as the overpass time moves later, which interferes with the estimation of long-term changes in the surface properties, such as, vegetation conditions, albedo, because the changing angle of solar incidence causes variation in observed radiances as the AVHRR scans the earth [11]. Therefore, data for these years are considerably stable compared to data for other years. That is why these data were considered as the standards for the normalized data.

Empirical Distribution Function (EDF) Technique for Normalization of Satellite Data

EDF approach is based on the physical reality that each ecosystem may be characterized by very specific

statistical distribution, independent of the time of observation. It is the best available technique to normalize satellite data. It allows us to represent global ecosystem from desert to tropical forest and to correct extreme distortions in satellite data related to technical problem.

To generate the normalized data, the proposed method begins with selection of samples of un-normalized earth-scene data covering as much of the range of intensities as possible. For NOAA satellites, the area is rectangular, extending several thousand pixels from desert to tropical forest (both east to west and north to south). Corresponding to the incoming radiance from any pixel, the instrument responds with an output x in digital counts. One can compile the discrete density function, i.e., the histogram, describing the relative frequency of occurrence of each possible count value for each year. For the i th year, let the histogram be $P_i(x)$. An EDF $P_d(x)$ can then be generated using the following relation [12], [14].

$$P_d(x) = \sum_0^x P_i(x) \quad (5)$$

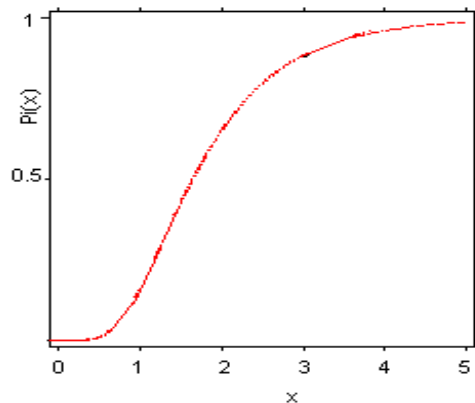


Fig. 2. Empirical distribution function [12]

The EDF is also known as a cumulative histogram of relative frequency, which is a non-decreasing function of x with a maximum value of unity as depicted in Fig. 2. The basic premise of normalization is that for each output value x in the i th year, the normalized value x' should satisfy the empirical relation given by

$$P_s(x') = P_d(x) \quad (6)$$

where the subscript s refers to the standard year. In practice, not only is P_s non-decreasing, but it is also monotonically increasing as a function of x' in the domain of x' where there are data. Therefore, it can be inverted, yielding the solution for x' as follows

$$x' = P_s^{-1}(P_d(x)) \quad (7)$$

When it is applied sequentially for every possible count value x , Eq. (7) generates the normalized data relating each x to an x' . Fig. 3 demonstrates how the procedure can be applied in practice to generate the

normalized data [12], [14]. Idealized EDFs are shown in the figure for the i th standard and un-normalized year. Though the EDFs are shown to be continuous, but in practice they can be discrete, being specified only integer values of x . To find x_1 , the normalized count value corresponding to the un-normalized count value of x_1 , the following procedure needs be employed using Fig. 3.

- For the count value of x_1 in an un-normalized i th year, find the decimal or percentage value from the EDF of the i th year, which is shown as $P_i(x_1)$.
- Find the point on the standard year's EDF with the same decimal or percentage value. As per Eq. (6), that decimal or percentage can also be expressed as $P_s(x'_1)$.
- Finally, use the EDF of the standard year to find the normalized count value of x'_1 . Since the data are actually discrete, we needed to interpolate within the EDF of the standard year to find the value x_1 .

After normalization of satellite data, some errors were observed that the EDFs of un-normalized i th year and the standard years were not identical. The error is measured as the differences between the EDF of the standard and the un-normalized years and expressed in counts or percent.

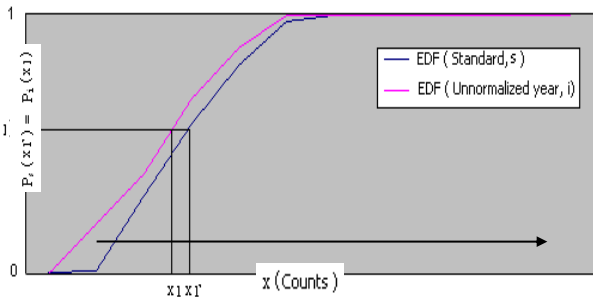


Fig. 3. Procedure to generate normalized data [12]

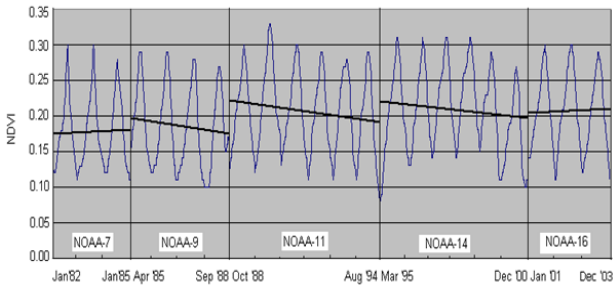


Fig. 4. NDVI time series (yearly old NDVI data) for study area China

VI. RESULTS and DISCUSSION

A. Analysis of NDVI Time Series for Study Area in China

NDVI time series data of five NOAA satellites were evaluated as shown in Fig. 4. Data from the afternoon polar orbiters is preferred for yielding the NDVI time series because of the high sun elevation angle (low solar zenith angle). However, the time it takes to cross the equator drifts to a later hour as the satellites age [3], [7], [8]. Satellite orbit drift results in a systematic change of illumination conditions which is one of the main sources of non-uniformity in multi-annual NDVI time series

Fig. 4 shows that the NDVI data of 1988, 1992, 1993, 1994, 1995 (week # 1-8), and 2000 are non-uniform as compared to other years because of satellite orbital drift, and sensor degradation. Therefore, the proposed EDF technique was applied to correct data of those years compared with standard year's data. First, the EDF for the un-normalized data were constructed which is then used to generate the normalized data compared with standard. Fig. 5 demonstrates how the procedure can be applied in practice to normalized NDVI value [12], [14]. The idealized EDFs for the standard year and for the year of 1988 are shown in the figure. As EDFs are based on cumulative histograms, they are supposed to be discrete quantities. However, they resemble a continuous function as can be obvious from Fig. 5. For example, for the NDVI value of 0.16 in the year of 1988, the EDF value was found to be 0.6. We can find the point on the standard data correction sets as well as evaluate the EDF value using Eq. (6) which also results in a value of 0.6. Finally, the EDF of the standard data correction was utilized to find the normalized count value as 0.18. Since the data are actually discrete, the EDF of the standard data correction sets needs be interpolated to find the value of 0.18. Therefore, the new NDVI value for the year of 1988 is $[NDVI_{1988} + (NDVI_{standard} - NDVI_{1988})]$ which yields $0.16 + (0.18 - 0.16) = 0.18$. Using this technique, EDFs produce the normalized or corrected data for the year of 1988 (new 1988 NDVI data) compared with standard year's data which are illustrated in Fig. 6. Similarly, we normalized data for the years of 1992, 1993, 1994, 1995 (week# 1-8), and 2000 compared with standard years' data using the proposed technique. The normalized data were used to produce new NDVI time series for the study area in China. Fig. 7 shows the improvement in the NDVI data (pink line) for the years of 1988, 1992, 1993, 1994, 1995, and 2000.

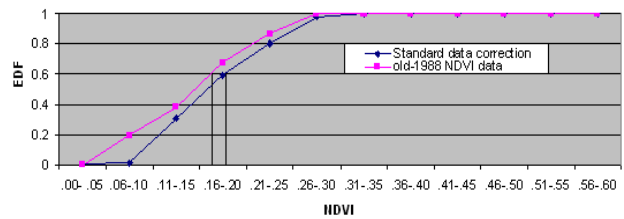


Fig. 5. Procedure to generate normalized NDVI data in 1988

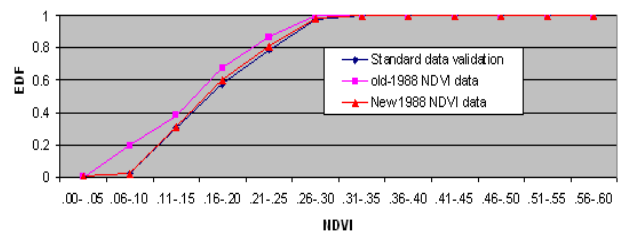


Fig. 6. EDFs for normalized data of 1988 compared with standard data

NDVI trends for China and the jumps between the satellites are illustrated in Fig. 7 and the errors are estimated as listed in Table I using Eqs. (3) and (4). Considering old NDVI trends (Table I), for China,

NOAA-9, -11, and -14 have negative trends and NOAA-7, -16 have positive trends. Therefore, NOAA-7, and -16 show clear tendency to NDVI increase during its three years in operation. However, the more important features here are the trend rates. The analysis shows that the high rate of NDVI change for NOAA-9, -11, and -14 by reduction of NDVI in 1988, 1992-1994, and 2000, are due to considerable degradation of satellite orbit. Regarding the NDVI jump from one satellite to the next in Table I (Column B), the general tendency is a reduction of NDVI between the beginning of NOAA-9 and the end of NOAA-7, and between the beginning of NOAA-16 and the end of NOAA-14. An increase in NDVI is observed only during satellite change from NOAA-9 to NOAA-11, NOAA-11 to NOAA-14, and NOAA-14 to NOAA-16, and is due to the orbit drift of the satellite. After correction of NDVI data, the errors of NDVI trends and jumps between the satellites were also computed and listed in Table I. The results in Table I show improvement of the NDVI trends for each satellite and the jump from one satellite to the next one. But there remain other potential sources of error in the NDVI data,

such as, an incomplete drift correction, and inaccurate NDVI calculation. The EDF method was designed to reduce errors due to orbit drift and the dominant uncertainty in temperature variation during the satellite life time.

TABLE I. ESTIMATION OF ERRORS IN (A) NDVI TREND AT THE END OF A SATELLITE LIFE AND (B) JUMPS BETWEEN THE SATELLITES (% TO THE BEGINNING LEVEL)

Target		A					B			
		N-7	N-9	N-11	N-14	N-16	N-7/9	N-9/11	N-11/14	N-14/16
China	Old NDVI	3	-10	-12	-11	7	10	30	16	5
	New NDVI	3	-5	0	0	7	7	19	0	-5

However, it may be difficult to accurately and completely remove this effect and hence the orbit remains as an error source, though at a reduced level. Another large uncertainty lies in the NDVI calibration which includes all errors, such as, incomplete atmospheric corrections, surface corrections, and sensor degradation.

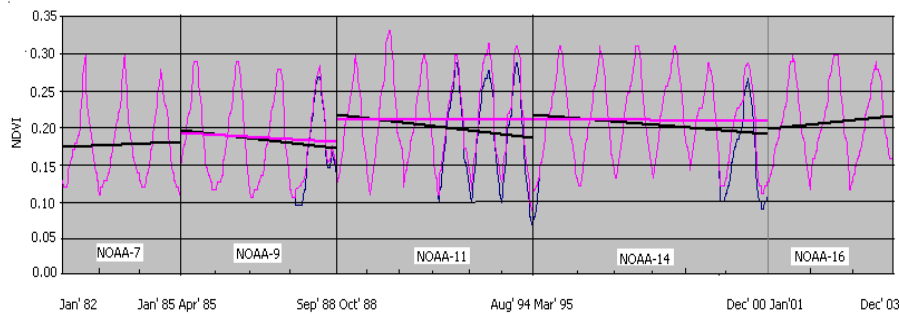


Fig. 7. New NDVI time series (yearly) in China (old NDVI data — , new NDVI data —)

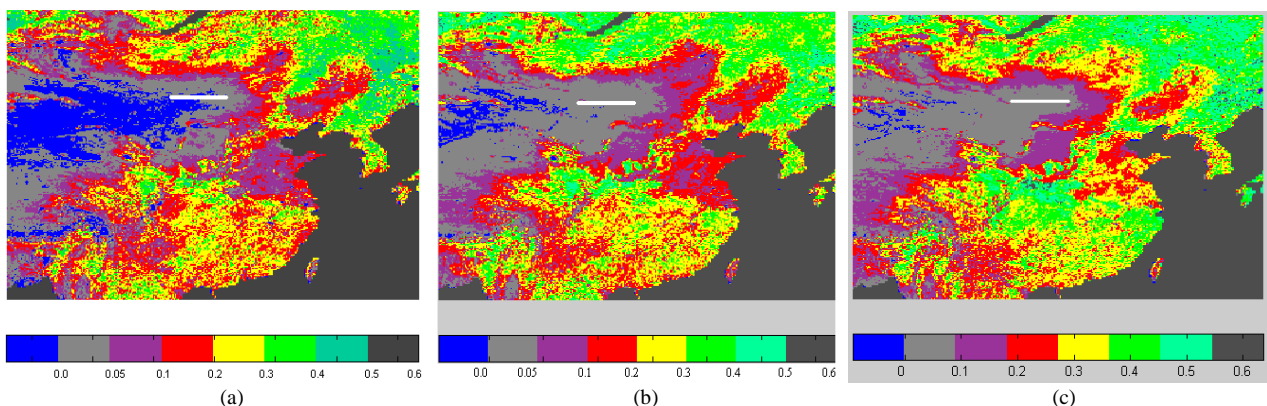


Fig. 8. NDVI image of: (a) old NDVI in week number 26 of 1988, (b) old NDVI (corrected data) in week number 26 of 1988, (c) standard in week number 26 of 1988

B. Analysis of NDVI Image for Study Area in China

Fig. 8 shows the NDVI image of week number 26 (end of June) of the year of 1988, which was visually checked for navigation accuracy, remapped if necessary, and assembled into a time series data. It also shows various ecosystems in China, such as, desert, grassland, forest, and mixed, based on the range of NDVI data. Desert targets are designated in both gray and purple. Vegetative targets include grassland, forest (broadleaf, coniferous

and tropical) ecosystems, and crop areas, which are designated in green and yellow. Blue indicates water, soil, and rock, and red represents mixed fields between deserts and vegetative. Fig. 8(b) shows an example of the corrected NDVI image, which is similar to the standard NDVI image of Fig. 8(c).

It can observe from Fig. 8 (b) that over China the value of NDVI significantly improved after correction of week number 26 of 1988. Small increases are observed in the tropical forest area. Although the overall corrections are

reasonable, fine straight lines are observed in Fig. 8 over certain areas, including desert and water. It can also be obvious from these figures that the corrected NDVI distribution appears reasonable, suggesting that the

artificial lines noted in this figure, while undesirable, do not cause significant error on the corrected NDVI value and, therefore, the corrected data may still be useful for further study or application.

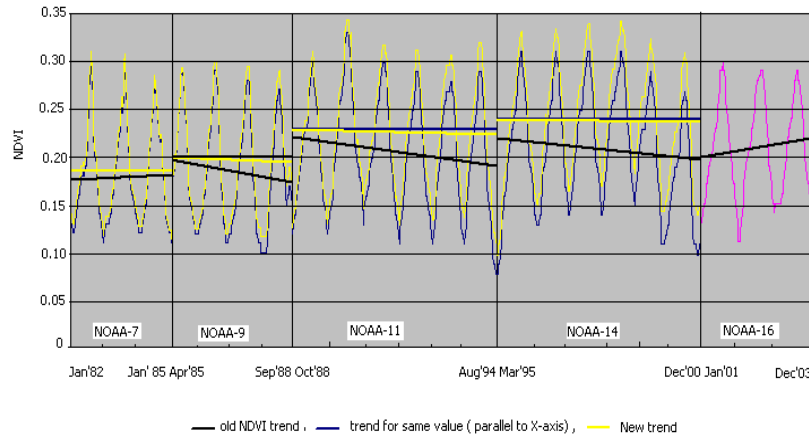


Fig. 9. Corrected NDVI time series (yellow line) by the trend estimation method (based on consistent value)

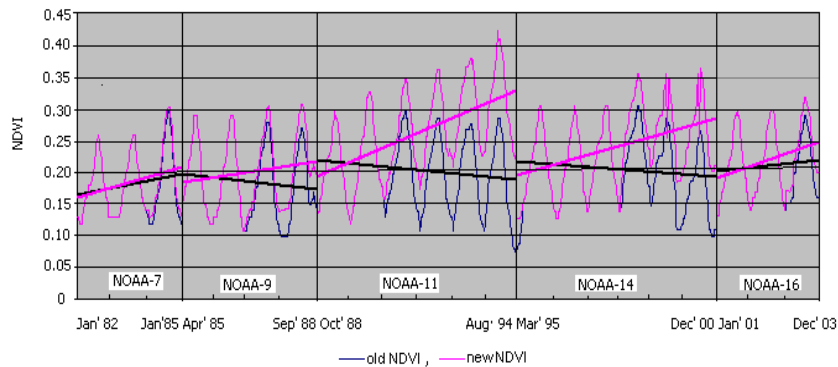


Fig. 10. Corrected NDVI time series (pink line) by the trend estimation method (based on standard years)

C. Comparison of EDF with Other Methods

1) Method 1: Trend estimation based on consistent value

Performance of the proposed EDF method was compared with that of the trend estimation method for the correction of satellite data. Given the monotonic decrease in reflectance, it was chosen to fit a trend line to the NDVI data (parallel to the X-axis), using the monitor output from NOAA-7 (January 1982- January 1985), NOAA-9 (April 1985 - September 1988), NOAA-11 (October 1988-August 1994), and NOAA-14 (March 1995-December 2000) satellites. The trend lines were derived for the un-normalized NDVI values for each satellite. The degradation trends were normalized by comparing with the trend which is a straight line in Fig. 7 for each week of each satellite. For example, the un-normalized NDVI value of the week number 18 of 1988 is 0.18. First, the NDVI value was determined for the same week on the trend straight line, which was found to be 0.20. Then the difference of two NDVI values for the same week was estimated as 0.02. Thus the normalized NDVI value for that week was determined by adding 0.2 to 0.18. Similarly, the NDVI value for the weeks of NOAA-7, NOAA-9, NOAA-11, and NOAA-14 were normalized. Finally, the new NDVI time series data were

calculated using the new values of each satellite. Fig. 9 shows the new NDVI for each satellite (yellow line).

The NDVI values of NOAA-16 satellites were not normalized using this method because these satellites did not have a trend. Fig. 7 shows the comparative performance of the proposed technique and the trend estimation method. It can be obvious from the figure that the EDF method performs better because the trend estimation method corrects all years' data. Also the EDF Method does not need to correct the first two years for each satellite since the first two years produced data of good quality. Therefore, the EDF method was used to correct satellite data in this study because the normalized data are relatively closer to the standard data. In addition, unlike with the trend estimation method, the proposed method does not need to correct all years' data.

2) Method 2: Trend estimation based on standard years

The trend equation was estimated for the first two years (104 weeks) of each satellite's life because these years were considered as standards. The number of weeks is plotted along the X-axis while the Y-axis contains the NDVI value. Next, the trend equation was calculated for a number of total weeks of each satellite. For example, the total weeks of X=183 were used for NOAA-9 (April

1985- September 1988) to find the trend equation of that satellite. The decline trend for old NDVI value of each satellite was also derived. Then the decline trend was normalized by comparing it with the trend equation based on standard years of each satellite. For example, the old NDVI value of the week number 26 of 1988 is 0.25. First, the NDVI value for the week number 169 was calculated by using the old NDVI trend equation $asy = -0.0001x + 0.1983$, $x = 169$, which resulted in a value of 0.18. Second, the NDVI value was estimated for the same week by using the trend equation as $y = 0.0003x + 0.1705$, $x = 169$, based on standard years (1985 and 1986). The estimated NDVI value is 0.22. Then the difference of two NDVI values for the same week was estimated as 0.04. Finally, the normalized NDVI value for that week was determined by adding 0.04 to 0.25. Similarly, the NDVI values were normalized for each week of NOAA-7, NOAA-9, NOAA-11, and NOAA-14 except for the standard years. The new NDVI time series data were derived using the new value of each satellite and shown in Fig. 10 (pink line). The main disadvantage of that method is that there is a bigger shift between estimated data from any two satellites during transition between satellites. Consequently, data for all years are shifted except for the standard year which is not desirable. Therefore, the EDF method was used to correct the satellite data of Fig. 7 in this study because normalized data are relatively closer to the standard data. In addition, the EDF method does not need to correct all years' data.

VII. CONCLUSIONS

The behavior of 22 year NOAA/NESDIS global vegetation index (GVI) data were analyzed in this paper to eliminate the long-term error of the NDVI data in China data set, because it includes a wide variety of different ecosystems represented globally. To correct this error, some possible techniques were considered, including empirical distribution functions, and trend estimation methods based on consistent value, and the standard years, respectively. The analytical performance of the techniques was compared to those of the most optimum EDF. Based on the simulation results of the normalization of AVHRR data in this study, it can be obvious that the proposed EDF method yields more accurate and effective performance than other methods. The main disadvantage of other methods is that they correct data for all the years. On the other hand, the EDF Method does not need to correct data for the first two years for each satellite since the first two years produce data of good quality. In addition, the EDF method offers an exact technique for satellite data normalization which depends on an adequate sample size for the approximations to be valid. Therefore, the EDF method was used to correct satellite data in this study because normalized data are relatively closer to the standard data. These analyses and results provide strong support to the

contention that normalization by EDF is a more efficient method for eliminating the drift effect and sensor degradation.

Despite these advantages, the EDF technique has a couple of limitations, including limited resolutions by the available representative sample. Perhaps the most serious limitation is that the distribution must be fully specified, which means that if the location, scale, and shape parameters are estimated from the data, the critical region of the EDF technique is no longer valid. Typically, it should be determined by simulation. In addition, EDFs are only applicable to continuous distribution. EDF provide the best metric by approximating probabilistic distribution of the sample at hand. Error exists when EDFs of the un-normalized year and the standard data validation years are not identical.

The proposed EDF approach shows encouraging results which can be used globally to create vegetation index to improve climatology. This method can also be derived from satellite observations, such as, GOES, assuming the retrievals have proven quality. The correction of NDVI images was found to be excellent. The AVHRR data were derived from seven-day composites using days when the maximum and minimum NDVI occurs. Therefore, the dataset containing the seven-day AVHRR data composites may itself be discrete. The line evident in the correction term seems to be more related to the standard, which suggests that the dataset may still be useful in climate studies.

ACKNOWLEDGMENT

The authors would like to thank Dr. Felix Kogan, NOAA/NESDIS, MD, USA, for providing the data and for his support and guidance during this work.

REFERENCES

- [1] H. Yin, T. Udelhoven, R. Fensholt, D. Pflugmacher, and P. Hostert, "How normalized different vegetation index (NDVI) trends from advanced very high resolution radiometer (AVHRR) and system probatoire d'observation de la terre vegetation (SPOT VGT) time series differ in agricultural areas: An inner Mongolian case study," *Remote Sensing*, vol. 4, pp. 3364-3389, 2014.
- [2] J. R. Nagol, E. F. Vermote, and S. D. Prince, "Quantification of impact of orbital drift on inter-annual trends in AVHRR NDVI data," *Remote Sensing*, vol. 6, pp. 6680-6687, 2014.
- [3] A. Devasthale, K. G. Karlsson, J. Quaa, and H. Grassl, "Correcting orbital drift signal in the time series of AVHRR derived convective cloud fraction using rotated empirical orthogonal function," *Atmospheric Measuring Technique*, vol. 5, pp. 267-273, 2012.
- [4] F. N. Kogan, T. Adamenko, and W. Guo, "Global and regional drought dynamics in the climate warming era," *Remote Sensing Letters*, vol. 4, no. 4, pp. 364-372, 2013.
- [5] F. N. Kogan and X. Zhu, "Evolution of long-term errors in NDVI time series: 1985-1999," *Advances in Space Research*, vol. 28, no. 1, pp. 149-153, 2001.
- [6] G. Gutman and Garik, "The use of long-term global data of land reflectances and vegetation indices derived from the AVHRR," *Journal of Geophysical Study*, vol. 104, no. 6, pp. 6241-6255, 1999.

- [7] J. C. Price, "Timing of NOAA afternoon passes" *International Journal of Remote Sensing*, vol. 12, pp. 193-198, 1991.
- [8] A. Ignatov, I. Laszlo, E. D. Harrod, K. B. Kidwell, and G. P. Goodrum, "Equator crossing times for NOAA, ERS and EOS sun-synchronous satellites," *International Journal of Remote Sensing*, vol. 25, no. 23, pp. 5255-5266, 2004.
- [9] J. R. Dim, H. Murakami, T. Y. Nakajima, B. Nordell, A. K. Heidinger, and T. Takamura, "The recent state of the climate: Driving components of cloud-type variability" *Journal Of Geophysical Research*, vol. 116, 2011.
- [10] K. B. Kidwell, *Global Vegetation User's Guide*, U.S. Department of Commerce, National Oceanic and Atmospheric Administration, Satellite Data Services Division, Maryland: Camp Spring, 1997.
- [11] J. A. Sobrino, Y. Julien, M. Atitar, and F. Nerry, "Noaa-AVHRR orbital drift correction from solar zenithal angle data," *IEEE Transactions on Geoscience and Remote Sensing*, vol. 46, no. 12, 2008.
- [12] M. Vargas, F. Kogan, and W. Guo, "Empirical normalization for the effect of volcanic stratospheric aerosols on AVHRR NDVI," *Geophysical Research Letters*, vol. 36, 2009.
- [13] AVHRR Polar Pathfinder Twice-Daily 5 km EASE-grid Composites. (July 20, 2014). [Online]. Available: http://nsidc.org/data/docs/daac/nsidc0066_avhrr_5km.gd.html
- [14] M. Vargas, *et al.*, "Statistical normalization of brightness temperature records from the NOAA/AVHRR," in *Proc. SPIE 8156, Remote Sensing and Modeling of Ecosystems for Sustainability VIII*, vol. 8156, 2011.



Md. Z. Rahman received his Bachelor in Electrical Engineering from Bangladesh University of Engineering and Technology (BUET), Master's and Ph.D. from the City University of New York, New York, USA. His major field of studies in the error correction of NOAA/GOES environmental satellite data due to orbital drift, sensor

deterioration and/or synchronization satellite remote sensing, and application of NOAA environmental satellite data such as climate and weather impact on ecosystems. Currently, he is an Associate Professor in the Mathematics, Engineering and Computer Science Department at LaGuardia Community College of the City University of New York. He is also a registered Professional Engineer in the states of New York and Michigan. He received a NASA research grant and PSC-CUNY research grant. Dr. Rahman is an active member of IEEE, SPIE, AMS, IEB, and CCPE. In the past years, he published more than 15 papers in refereed journals and conference proceedings.



L. Roytman is a Professor in the Electrical Engineering Department at City College of New York. He has been a faculty member at CCNY since 1984. His research interests are Satellite Remote Sensing Applications, Vegetation Health and its Application for Vector borne Diseases and Agriculture. He published more than 105 research article in refereed journals and conference proceedings.

He has acted as Principle Investigator of numerous national and international U projects funded by the NOAA, NASA, NSF, and USAID . USAID. He is a Fellow member of IEEE.



M. Nazrul Islam is an Associate Professor at SUNY – Farmingdale. He also worked at Old Dominion University, University of South Alabama, University of West Florida, and Bangladesh University of Engineering and Technology. He published more than 140 publications in refereed journals and conference proceedings. His research interests include optical communication, wireless communication, digital image processing and solid state devices. He is a Senior Member of SPIE and a Senior Member of IEEE.